THE STRUCTURES OF THE MINERALS OF THE DESCLOIZITE AND ADELITE GROUPS: IV—DESCLOIZITE AND CONICHALCITE (PART 2) THE STRUCTURE OF CONICHALCITE

M. M. QURASHI[1] AND W. H. BARNES

Division of Pure Physics, National Research Council, Ottawa, Canada

ABSTRACT

The structure of conichalcite $CaCu(AsO_4)(OH)$, has been refined first in *Pnma* by two-dimensional partial-difference syntheses, followed by antisymmetrical Patterson and Fourier syntheses, utilizing a number of observed reflections forbidden in *Pnma*, and finally in $P2_12_12_1$ by difference syntheses in which all observed reflections have been included. The structure consists of a three-dimensional assemblage of distorted AsO_4 tetrahedra, $CuO_4(OH)_2$ tetragonal bipyramids, and $CaO_7(OH)$ square antiprisms, sharing corners and edges. The possible significance of the two types of bond lengths in the AsO_4 group is discussed.

INTRODUCTION

Conichalcite, $CaCu(AsO_4)(OH)$, was assigned to space group *Pnam* by Berry (1951), but, for direct comparison with descloizite, $Pb(Zn, Cu)(VO_4)(OH)$, and pyrobelonite, $PbMn(VO_4)(OH)$, (Barnes & Qurashi, 1952), it is more convenient to interchange b and c and use the standard orientation for D_{2h}^{16}, namely, *Pnma*. On this basis, $a = 7.40$ Å, $b = 5.84$ Å, $c = 9.21$ Å, $Z = 4$ (Berry, 1951). Later, the space group was shown to be $P2_12_12_1$ (Qurashi, Barnes & Berry, 1953) with the observation of several weak $0kl$ reflections for which $k + l = 2n + 1$ and a few very weak $hk0$ reflections for which $h = 2n + 1$. By ignoring these reflections, however, it was possible to deduce an approximate structure for conichalcite in *Pnma* with the aid of a preliminary structure for descloizite (Qurashi & Barnes, 1954). It was shown that Ca, Cu, and As occupy sites in the lattice of conichalcite which correspond with those occupied by Pb, (Zn, Cu), and V, respectively, in the lattice of descloizite. The trial structure for conichalcite has now been refined in *Pnma*, and finally in $P2_12_12_1$ with the introduction of the appropriate antisymmetrical atomic displacements necessary to account for the presence of the weak reflections previously ignored.

REFINEMENT IN *Pnma*

Refinement of the approximate structure for conichalcite (Qurashi & Barnes, 1954) was commenced in *Pnma* because the 0kl Fourier map acquires pseudo-reflection symmetry about $y = 0$ as a result of the fact that calcium and arsenic differ comparatively little in atomic scattering power. The signs of all reflections for which $k = 2n + 1$, therefore, are not determined by the metal atoms alone, but are dependent also on the disposition of the oxygen atoms. Two cycles of refinement for each of the three principal zones were carried out by $(F_o - F_{c(m)})$ — syntheses, where $F_{c(m)}$ represents values of F calculated for the metal atoms alone. The final partial difference maps are shown in Fig. 1. Mean values of the atomic co-ordinates at this stage were Ca at $0.122, \frac{1}{4}, 0.174$, Cu at $0, 0, \frac{1}{2}$, As at $0.372, -\frac{1}{4}, 0.329$, O_1 at $0.180, -\frac{1}{4}, \frac{1}{2} - 0.052$, O_2 at $0.536, -\frac{1}{4} \pm 0.09, \frac{1}{2} - 0.054$, $O_3(O_4)$ at $0.370, -0.006, 0.234$, and O_5 at
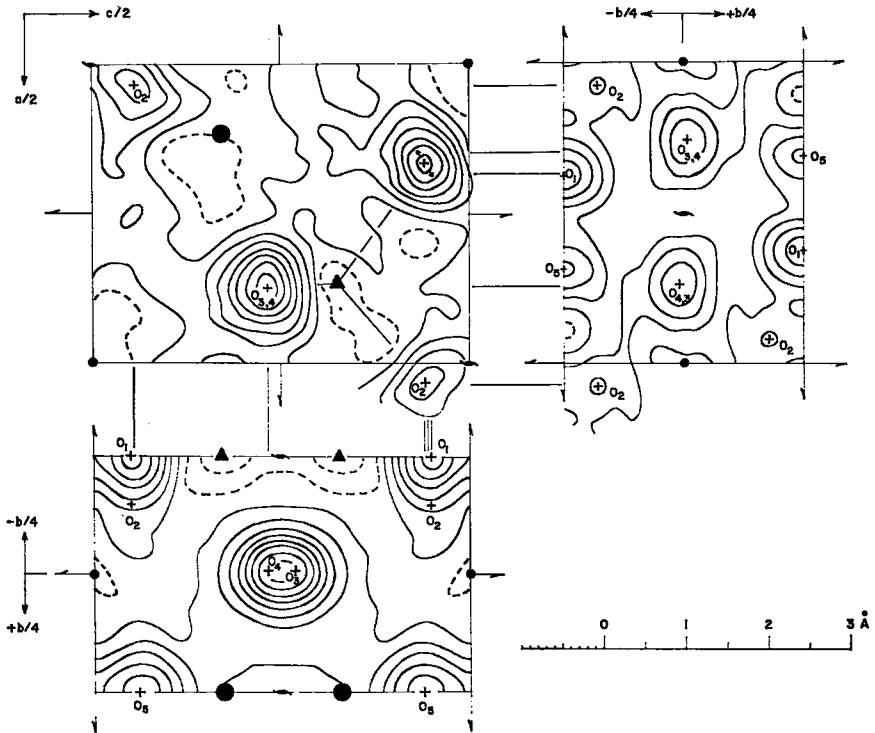

FIG. 1. Partial difference maps after preliminary refinement in *Pnma*. Large solid circles, Ca; small solid circles, Cu; triangles, As; crosses, O; Contours at intervals of 2 $e.\text{Å}^{-2}$; zero and negative contours indicated by broken lines.

0.162, $\frac{1}{4}, \frac{1}{2}$ — 0.064. These sites are very close to those of Pb, Mn, V, and the five O, respectively, in pyrobelonite (Donaldson & Barnes, 1955), and to those of Pb, (Zn, Cu), V, and the five O, respectively, in the unrefined structure of descloizite (Qurashi & Barnes, 1954). Inspection of Fig. 1, however, suggests very strongly that O_2 should be displaced (as indicated) by about $0.09b = 0.5$ Å from the special position at $y = \frac{1}{4}$ which it should occupy in *Pnma;* otherwise, no other departures from *Pnma* symmetry are obvious. It is of interest to note that similar separations of O_1 and O_5 in the $h0l$ and $hk0$ maps of Fig. 1 appear in corresponding maps for pyrobelonite (Donaldson & Barnes, 1955), but the possible difference between the x co-ordinates for O_3 and O_4 noted in pyrobelonite is not apparent in the present Fig. 1. The R-factors were approximately 0.09_5 for the $hk0$, 0.14 for the $h0l$, and 0.20 for the $0kl$ reflections. The last two values were not very satisfactory, and for a number of individual reflections, particularly $0kl$, there were relatively large discrepancies between $|F_o|$ and F_c. These results indicated, therefore, that the effect of the departure of some of the atoms from the special positions of *Pnma* must partially cancel out in the case of the $hk0$ reflections but are cumulative for the $0kl$ reflections. Attempts to improve the agreement between $|F_o|$ and F_c by combinations of shifts of the sites of the oxygen atoms alone led to the conclusion that at least some of the heavier atoms also must be displaced from their *Pnma* positions, and that a systematic examination of the antisymmetrical components of the Patterson maps might be of assistance.

THE NON-*Pnma* REFLECTIONS AND THE ANTISYMMETRICAL PATTERSON MAPS

The Patterson map, derived from data for those $0kl$ reflections for which $k + l = 2n$, is symmetrical about a line joining $(-, 0, 0)$ and $(-, \frac{1}{2}, \frac{1}{2})$, whereas that derived from data for the non-*Pnma* $0kl$ reflections (those for which $k + l = 2n + 1$) is not. Thus, each of the Patterson peaks, P_o, based on all the observed data, must consist of a super-symmetrical part, P_s, and an antisymmetrical component, ΔP, which is relatively small in the present case, and $P_o = P_s + \Delta P$. Therefore, while the interpretation of P_s alone leads to the ideal atomic positions of *Pnma*, analysis of ΔP should yield quantitative estimates of the actual departures of the atoms from the positions of higher symmetry. The mathematical treatment of this concept is discussed elsewhere (Qurashi, 1963). When the atomic displacements from *Pnma* positions are small, the magnitudes of the peaks and troughs in the two-dimensional ΔP maps are proportional to the squares of the displacements, Δ^2, and approximately to the squares of the atomic numbers, Z^2, of the atoms

concerned, and the heights of the origin peaks are proportional to $\Sigma(Z\Delta)^2$ summed over all the atoms.

Making use of $|F_o|$ for only those observed reflections which are forbidden in *Pnma*, the $0kl$ and $hk0$ ΔP functions were evaluated and the resulting maps are reproduced in Fig. 2. Possible displacements from *Pnma* positions which would affect the ΔP maps are limited to the y direction for Ca, As, O_1, O_2, and O_5, and to both y and z for Cu; there are no restrictions on any of the co-ordinates of O_3 and O_4 in either *Pnma* or $P2_12_12_1$ but the two atoms are symmetrically equivalent in the former and not in the latter.
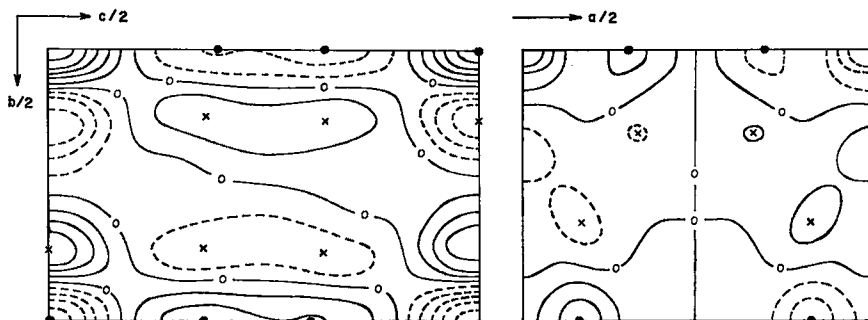

FIG. 2. Antisymmetrical Patterson ΔP-maps. Contours at intervals of 0.5 units in the $0kl$, and 0.25 units in the $hk0$, map, with zero contours indicated by 0's and negative contours by broken lines. The small solid circles mark the positive and negative non-origin peaks and the crosses show the corresponding negative and positive regions.

No displacement of Cu from $y = 0$, $z = 0$ is indicated by the ΔP maps. A displacement along b from $y = 0$ would make contributions of opposite sign to the peaks at $(-, 0, 0)$ and $(-, 0, \frac{1}{2})$ but the observed heights of these peaks (Fig. 2) are almost the same (2.98 units and 2.42 units, respectively). Furthermore, a displacement along c from $z = 0$ would produce a negative self-interaction peak along c but no trough appears in the contours of the origin peak in the $0kl$ map of Fig. 2. Thus any departure of Cu from the *Pnma* positions at $(0, 0, \frac{1}{2}; 0, \frac{1}{2}, \frac{1}{2}; \frac{1}{2}, 0, 0; \frac{1}{2}, \frac{1}{2}, 0)$ must be negligibly small, and the main contributions to the ΔP maps must come from the atoms along $y = \pm\frac{1}{4}$, or from the oxygen atoms (represented by O_3 and O_4) in the eight-fold general positions of *Pnma*.

Examination of the $hk0$ map in Fig. 2 shows that the positive and negative non-origin peaks occur at $(\frac{1}{6}, 0, -)$ and $(\frac{1}{12}, \frac{1}{2}, -)$, and these must arise from antisymmetrical displacements along the direction of y of some, or all, of those atoms (Ca, As, O_1, O_2, O_5) placed at $y = \pm\frac{1}{4}$ in *Pnma*. Attention, therefore, may be directed towards these atoms, and

an examination of the equivalence or non-equivalence of O_3 and O_4 may be left for the final refinement in $P2_12_12_1$. A striking feature of the ΔP maps (Fig. 2) is the difference between the heights of the $0kl$ origin peak (2.98 units) and the $hk0$ origin peak (0.92 units). If two atoms have

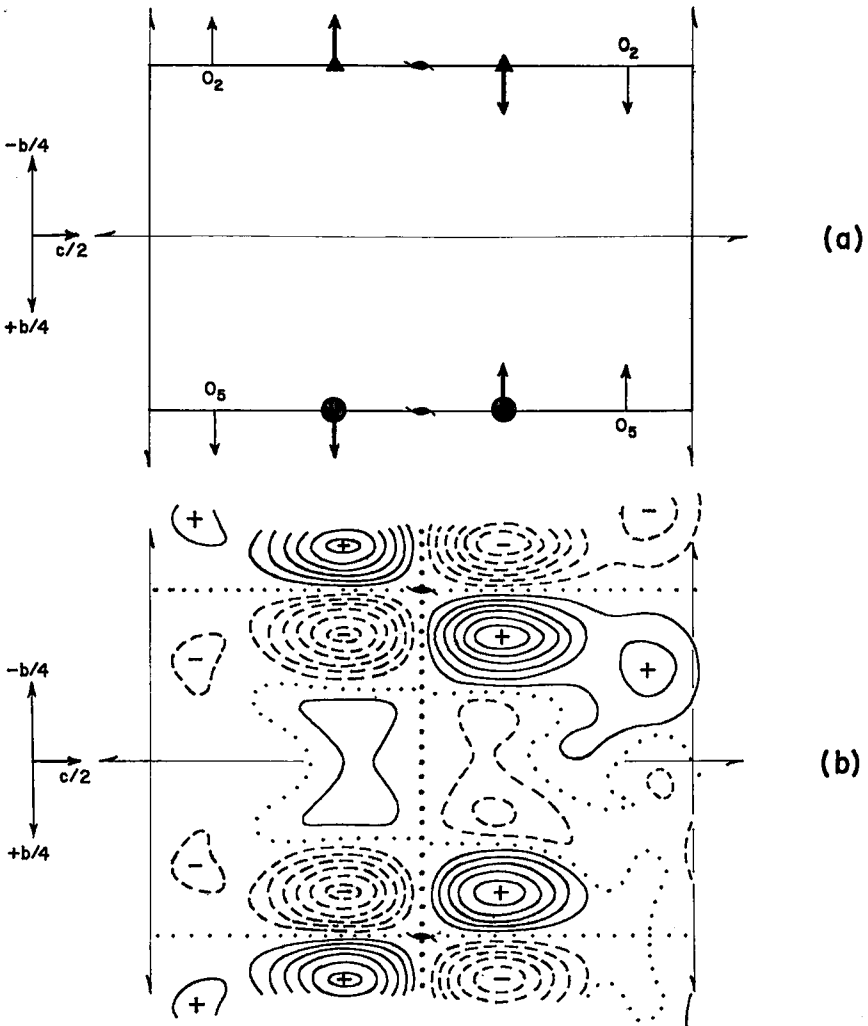FIG. 3(a) Directions of the antisymmetrical shifts of Ca (large solid circles), As (triangles), O_2, and O_5, deduced from the ΔP-maps.

(b) *Left*, antisymmetrical Fourier synthesis omitting the 021 reflection; *right*, anti-symmetrical Fourier synthesis including the 021 reflection. Contours at intervals of $1e.\text{Å}^{-2}$, with zero contour dotted and negative contours broken.

opposite displacements and overlap in a given projection, their normal contribution, $(Z_1\Delta_1)^2 + (Z_2\Delta_2)^2$, to the origin peak becomes the much smaller quantity, $(Z_1\Delta_1 - Z_2\Delta_2)^2$. In the $hk0$ projection (Qurashi & Barnes, 1954, Fig. 8) there is one site, at $(\frac{1}{8}, \frac{1}{4}, 0)$, where Ca, As, and O_5 all overlap, whereas they are completely separated in the $0kl$ projection. The large difference (2.06 units) between the two origin peaks in the ΔP maps, which accounts for more than two-thirds of the total anti-symmetrical effect, must, therefore, be attributed to these three atoms, and probably to only two of them. It is evident from the initial refinement in *Pnma* that the largest displacement (see Fig. 1) almost certainly occurs for O_2, and thus most, if not all, of the $hk0$ origin-peak may tentatively be attributed to O_2 self-interactions.

The relative contributions of Ca, As, and O_5 to the remaining 2.06 units of the origin peak in the $0kl$ ΔP map may be estimated as follows, on the initial assumption that each is responsible for about 0.69 units. In order to produce the large negative interaction peak at $(-, \frac{1}{2}, 0)$ the two atoms of each of the pairs Ca, As and O_2, O_5 must have their shifts in opposite directions, as illustrated in Fig. 3(a), because, if this were not so, one interaction would cancel out the other. It is necessary, there-fore, only to determine the relative directions of the displacements of one member of each pair. Since nothing was known at this time about a possible shift of O_5, attention was centered on As, O_2. The interactions among Ca, As, O_2, and O_5 produce peaks at $(-, 0, z)$ in the $0kl$ map. The calculated heights of these peaks for the two possible directions of the shifts of As and O_2 are given in Table 1 together with the z co-ordinates and peak heights actually observed. It is apparent that relative displace-ments of the atoms with the oxygen shifts as represented in Fig. 3(a) would give rise to peaks in the $0kl$ map in good agreement with those observed, whereas the observed data are incompatible with the results to be expected if the relative directions of the shifts were to be reversed.

TABLE 1. $(-,0,z) = \Delta P$ PEAKS: HEIGHTS CALCULATED (1) FOR THE ARRANGEMENT OF FIG. 3 (a), CALCULATED (2) FOR THE REVERSED DIRECTION OF THE OXYGEN SHIFTS; AND THE HEIGHTS OBSERVED.

z	0.11	0.16	0.23	0.27	0.34	0.38	0.50
Ht. Calc. (1)	0.00	−0.75	−0.75	−0.75	−0.75	0.00	+2.75
			−1.1		−1.1		
Ht. Calc. (2)	−1.50	−0.75	+0.75	+0.75	−0.75	−1.50	+2.75
	−1.7		+1.1		−1.7		+2.75
Ht. Obs.			−1.02		−1.23		+2.42
z			0.19		0.32		0.50

In spite of imperfect resolution in the ΔP map it is significant that the positions of the compound peaks are closer to those calculated for metal-metal interactions than to those calculated for oxygen-metal interactions by an amount which suggests that $Z_m\Delta_m > Z_O\Delta_O$ by a factor of about 3/2, where the subscripts "m" and "O" refer to "metal" and "oxygen", respectively. On this basis an estimate of the magnitudes of Δ_m and Δ_O may be obtained from the height of the origin peak. Evaluation of the antisymmetrical Patterson function for the $0kl$ reflections forbidden in $Pnma$ gives

$$P(-, 0, 0) \approx 0.3[(Z_m\Delta_m)^2 + (Z_O\Delta_O)^2]$$
$$\approx 0.3(Z_m\Delta_m)^2[1 + 2/3]$$

so that, $\qquad\qquad 2.98 \approx 0.50(Z_m\Delta_m)^2$

and $\qquad\qquad Z_m\Delta_m \approx 2.4$

Similar values for $Z_m\Delta_m$ are obtained from the heights of the other peaks in the ΔP map. The mean value of $Z_m\Delta_m$ is 2.4 ± 0.2, from which $\Delta(As) = 0.07_3$ Å and $\Delta(Ca) = 0.12_0$ Å, and the mean value of $Z_O\Delta_O$ is 1.6, from which $\Delta(O) = 0.20$ Å.

ANTISYMMETRICAL FOURIER MAPS

Assuming, as before, that the contributions from the two atoms of each pair, As, Ca and O_2, O_5, are equal in magnitude (i.e., they have the same value of $Z\Delta$), the structure factor expressions for the non-$Pnma$ $0kl$ reflections are

$$F(As + Ca) \approx -16\pi k\hat{f}Z_m(\Delta_m/b) \sin 2\pi l(0.078), \text{ for } k = 2n + 1$$
$$= 0 \qquad\qquad\qquad\qquad , \text{ for } k = 2n$$

and,

$$F(O_2 + O_5) \approx -16\pi k\hat{f}Z_O(\Delta_O)/b) \sin 2\pi l(0.190), \text{ for } k = 2n + 1$$
$$= 0 \qquad\qquad\qquad\qquad , \text{ for } k = 2n$$

and,

$$F_c = F(As + Ca) + F(O_2 + O_5)$$

With the co-ordinates obtained as a result of the initial refinement in $Pnma$ and modified by the values for Δ deduced from the ΔP maps, and taking the directions of the shifts as represented in Fig. 3(a), structure factors calculated for the metal atoms only $(F_{c(m)})$, for the oxygen atoms only $(F_{c(O)})$, and for all four atoms $(F_{c(1)})$ are given in Table 2, together with the observed structure amplitudes $(|F_o|)$, for the eight non-$Pnma$

TABLE 2. COMPARISON OF $|F_o|$ FOR NON-$Pnma$ $0kl$ REFLECTIONS WITH
STRUCTURE FACTORS CALCULATED FOR ATOMIC DISPLACEMENTS FROM
$Pnma$ POSITIONS DERIVED FROM ΔP MAP: $F_{c(m)}$, FOR METAL ATOMS
ONLY; $F_{c(O)}$, FOR OXYGEN ATOMS ONLY; $F_{c(1)} = F_{c(m)} + F_{c(O)}$; $F_{c(2)}$,
WITH SHIFTS INDICATED BY ANTISYMMETRICAL FOURIER MAP

hkl	$F_{c(m)}$	$F_{c(O)}$	$F_{c(1)}$	$|F_o|$	$F_{c(2)}$
012	-14.7	$- 6.6$	-21	14	-16
021	0	0	0	21	-11
032	-31.6	-10.0	-42	48	-34
034	-30.7	$+11.6$	-19	34	-23
036	$- 5.7$	$- 6.6$	-12	23	$- 9$
038	$+16.3$	$+ 0.8$	$+17$	16	$+16$
052	-37.6	$- 9.1$	-47	41	-36
054	-38.3	$+12.5$	-26	34	-27

$0kl$ reflections observed. Taking $Z_m\Delta_m = (3/2)Z_O\Delta_O$, as indicated by the ΔP map, the signs of $|F_o|$ are controlled by the metal atoms for the reflections with $k = 2n + 1$ (see Table 2). Only one reflection, 021, violates the condition that $F_c = 0$ for $k = 2n$.

The antisymmetrical Fourier map, calculated with the data of Table 2, but omitting the contribution of the 021 reflection, is shown on the left-hand side of Fig. 3(b), where it is clear that the oxygen shifts constitute a relatively small part of the total antisymmetrical effect. The introduction of the 021 reflection, therefore, will have a marked influence on the apparent shifts because it will destroy the symmetry about $y = 0$, and will accentuate the peak corresponding to one oxygen atom while reducing that corresponding to the other. If $|F_o|$ for 021 is given the same sign as the relatively strong reflections 032 and 034, the Fourier map shown on the right-hand side of Fig. 3(b) is obtained, and it will be observed that a significant displacement of O_2 is indicated. This is in agreement with the results previously mentioned in connection with the $0kl$ and $hk0$ maps of Fig. 1. On the other hand, selection of the opposite sign for $|F_o|$ would produce an apparent shift for O_5 instead of O_2, and this in turn would reduce the ΔP $hk0$ map (Fig. 2) to the origin peak alone, because of the overlap of O_5, As, and Ca in the $hk0$ projection. Therefore, $|F_o|$ for the 021 reflection must be given the sign chosen for the calculation of the Fourier synthesis represented on the right-hand side of Fig. 3(b). The shifts estimated from this map are $\Delta(\text{As}) = 0.06$ Å, $\Delta(\text{Ca}) = 0.08$ Å, $\Delta(O_2) = 0.13$ Å, and $\Delta(O_5) < 0.03$ Å, which are in satisfactory agreement with those deduced from the ΔP maps. Taking the means of both sets, $\Delta(\text{As}) = 0.07$ Å, $\Delta(\text{Ca}) = 0.10$ Å, $\Delta(O_2) = 0.16$ Å, and $\Delta(O_5) < 0.03$ Å. Values of $F_{c(2)}$ calculated on the basis of these values are shown in Table 2, and are in sufficiently good agreement ($R = 0.27$) with the corresponding values of $|F_o|$ to justify final refinement of the whole structure in $P2_12_12_1$.

For this purpose all observed reflections were included, and the co-ordinates of As, Ca, and O_2 obtained from the initial refinement in *Pnma* were modified according to the foregoing displacements from their *Pnma* positions. In view of the small number of terms available for the anti-symmetrical Patterson and Fourier syntheses, however, these values for the shifts may be expected to be too low. No attempt was made to analyse the antisymmetrical data for possible displacements of O_1, O_3, and O_4 because the agreement between $|F_o|$ and $F_{c(2)}$ in Table 2 indicated that these shifts probably were small and might reasonably be expected to appear in the course of final refinement in $P2_12_12_1$.

FINAL REFINEMENT IN $P2_12_12_1$

The final refinement was carried out by means of difference syntheses, and the first cycle produced a striking reduction in R, for all the observed $0kl$ reflections, from 0.22 to 0.12, together with a decrease in the apparent temperature-factor constant from about 2 to 0.5. Improvements, although smaller, also were shown by the results for the $\{hk0\}$ and $\{h0l\}$ zones. With the inclusion of anisotropic temperature factors, three further cycles of refinement reduced R to 0.07_1, 0.06_6, and 0.05_2 for the $h0l$, $0kl$, and $hk0$ reflections, respectively, based on the observed data only, and to 0.09_6, 0.09_2, and 0.07_7, respectively, when the unobserved reflections (with $|F_o|$'s taken as one-half of the threshold values) were included.

The final fractional co-ordinates, referred to the *Pnma* origin are listed in Table 3 separately for the three principal zones, together with the mean value of each co-ordinate. For both Ca and As, the values of x and y derived from the $hk0$ data have been given one-half weight because of the overlap of these two atoms in the [001] projection. The root-mean-squares (r.m.s.) of one-half the differences between the two values of each co-ordinate for the five oxygen atoms collectively are $0.0068a = 0.050$ Å, $0.0048b = 0.028$ Å, and $0.0032c = 0.029$ Å. The

TABLE 3. FRACTIONAL ATOMIC CO-ORDINATES: *Pnma* ORIGIN

Atom	x			y			z		
	$\{hk0\}$	$\{h0l\}$	Mean	$\{hk0\}$	$\{0kl\}$	Mean	$\{h0l\}$	$\{0kl\}$	Mean
Ca	0.1220	0.1142	0.1168	0.2704	0.2692	0.2696	0.1762	0.1754	0.1758
Cu	0	0	0	0	0	0	$\frac{1}{4}$	$\frac{1}{4}$	$\frac{1}{4}$
As	0.3720	0.3668	0.3685	−0.2330	−0.2334	−0.2332	0.3313	0.3299	0.3306
O_1	0.186	0.188	0.187	−0.257	−0.255	−0.256	0.452	0.447	0.449_5
O_2	0.536	0.540	0.538	−0.166	−0.186	−0.176	0.446	0.442	0.444
O_3	0.370	0.387	0.378_5	0.506	0.512	0.509	0.234	0.244	0.239
O_4	0.376	0.359	0.367_5	−0.017	−0.014	$−0.015_5$	0.226	0.222	0.224
O_5 (OH)	0.161	0.141	0.151	0.250	0.250	0.250	0.426	0.433	0.429_5

TABLE 4. STRUCTURE FACTOR DATA SEPARATELY FOR THE
THREE PRINCIPAL ZONES ($P2_12_12_1$)

$0kl$	$|F_o|$	F_c	$0kl$	$|F_o|$	F_c	$0kl$	$|F_o|$	F_c
002	12	−7.6	024	156	−151.1	043	<14	−8.2
004	67	+67.7	025	<14	+1.3	044	40	+37.1
006	137	−142.2	026	44	−45.3	045	<14	−3.6
008	29	−35.2	027	<14	−0.5	046	116	−107.5
0.0.10	<14	−1.8	028	139	−137.4	047	<14	−1.5
011	41	+54.6	029	<14	+9.9	048	14	−16.9
012	14	−14.7	0.2.10	54	+54.5	051	24	+28.0
013	17	−16.8	031	19	+24.3	052	41	−44.5
014	<14	+1.7	032	48	−49.7	053	<14	+5.9
015	18	−16.9	033	<14	−9.1	054	34	−35.2
016	<14	+1.5	034	34	−32.3	055	21	−12.8
017	34	−39.6	035	33	−32.5	056	<14	−10.6
018	<14	+13.6	036	23	−21.0	057	21	−17.6
019	<14	+10.6	037	28	−26.9	060	18	+19.6
0.1.10	<14	+13.5	038	16	+14.2	061	<14	−7.8
020	83	+86.1	039	<14	+3.1	062	64	+61.4
021	21	−17.9	040	228	+223.8	063	<14	−6.3
022	80	+88.7	041	<14	−16.7	064	79	−72.0
023	<14	+0.2	042	<14	−1.1	065	<14	+0.4

$hk0$	$|F_o|$	F_c	$hk0$	$|F_o|$	F_c	$hk0$	$|F_o|$	F_c
020	83	−81.9	320	<12	−2.3	550	11	−12.3
040	228	+220.5	330	<12	−2.9	560	<12	−5.5
060	18	−21.7	340	<12	−4.2	600	84	−82.3
110	<12	−2.6	350	<12	−5.9	610	131	−125.7
120	18	+27.8	360	11	+15.2	620	36	−34.2
130	<12	−3.3	400	98	−97.1	630	91	+94.7
140	14	−17.5	410	<12	+10.6	640	62	−56.8
150	<12	+7.6	420	175	+173.9	650	74	−71.6
160	<12	+12.2	430	<12	−0.4	710	15	+6.7
200	91	−88.8	440	66	−66.2	720	<12	−6.0
210	166	+167.2	450	<12	−4.1	730	18	−8.5
220	93	−101.0	460	101	+97.8	740	11	+8.3
230	123	−124.8	510	<12	−7.0	800	119	+131.3
240	41	−43.0	520	<12	+0.8	810	<12	−4.5
250	95	+97.3	530	17	+18.2	820	24	−23.2
260	57	−55.9	540	<12	−0.8	830	12	+8.5
310	10	+2.6						

r.m.s. of the deviations for the three co-ordinates (converted to Å) for each oxygen atom separately are 0.012 Å for O_1, 0.036 Å for O_2, 0.044 Å for O_3, 0.036 Å for O_4, and 0.048 Å for O_5 (OH), with a mean of 0.035 Å. The corresponding weighted r.m.s. for Ca is 0.011 Å and it is 0.008 Å for As. The estimated standard deviations, calculated according to the formula of Cruickshank (1949), are 0.007 Å for Ca, 0.004 Å for As, and 0.020 Å for the five oxygen atoms. The means of both estimations are 0.009 Å for Ca, 0.006 Å for As, and 0.028 Å for O, from which the e.s.d.'s of the metal-oxygen distances are 0.029 Å for Ca—O, 0.028 Å for Cu—O, and 0.029 Å for As—O.

TABLE 4 (continued)

$h0l$	$|F_o|$	F_c	$h0l$	$|F_o|$	F_c	$h0l$	$|F_o|$	F_c
002	12	+9.3	209	23	+17.9	504	<14	+12.0
004	67	+68.3	2.0.10	40	+42.2	505	97	−93.9
006	137	+152.5	301	95	−87.2	506	<14	−3.8
008	29	−26.7	302	<14	+1.9	507	68	−67.7
0.0.10	<14	+6.6	303	31	+31.2	508	30	−40.0
101	52	−47.9	304	<14	−9.2	600	84	+81.1
102	46	+55.4	305	125	−118.8	601	40	−48.7
103	176	−191.4	306	23	−25.8	602	69	+62.1
104	18	+10.0	307	110	−107.9	603	<14	+5.7
105	19	−26.0	308	<14	+17.9	604	57	+47.8
106	<14	−5.5	309	<14	+10.6	605	<14	+11.1
107	23	−25.2	400	98	−94.9	606	46	+46.9
108	37	+40.1	401	25	−26.0	607	<14	−23.6
109	120	−119.8	402	178	+173.5	701	25	−24.1
1.0.10	26	−31.5	403	<14	+10.1	702	<14	+2.2
200	91	+93.3	404	104	+98.6	703	105	−107.9
201	65	+70.9	405	27	+24.3	704	<14	−9.6
202	95	+94.7	406	29	−25.0	705	<14	−8.6
203	75	−73.1	407	<14	−19.0	706	<14	+10.8
204	81	+82.9	408	107	+99.0	800	119	+123.4
205	40	−45.9	409	<14	+5.7	801	24	+29.5
206	59	+62.9	501	115	−107.2	802	<14	−12.4
207	<14	+9.3	502	58	−59.0	803	<14	−12.7
208	57	+52.2	503	<14	+1.1			

The calculated structure factors are compared with the observed structure amplitudes separately for the three principal zones in Table 4. The co-ordinates employed are those given for each zone in Table 3 but referred to the standard origins of the principal projections (pgg) of $P2_12_12_1$. The atomic scattering factors for As^{+2}, Ca^{+2}, and O^{-1}, given by Freeman (1959), and for Cu^{+2}, given by Watson & Freeman (1961) were adopted. The final temperature-factor constants for Ca, Cu, and As in each zone are shown in Table 5; an isotropic value of $B = 1.0$ was employed for each oxygen atom in all zones. The three metal atoms were treated anisotropically in the $\{0kl\}$ zone and isotropically in the other two zones as indicated in Table 5, where the mean values of B with the limits for the two anisotropic components are given under $\{0kl\}$. The anisotropy in this zone is greatest for copper and the direction of apparent maximum thermal vibration is perpendicular to the two Cu—OH bonds.

TABLE 5. TEMPERATURE-FACTOR CONSTANTS (B) FOR THE METAL ATOMS SEPARATELY IN THE THREE PRINCIPAL ZONES

Atom	$\{0kl\}$	$\{h0l\}$	$\{hk0\}$
Ca	0.2 ± 0.2	0.4	0.2
Cu	0.95 ± 0.5	0.6	0.7
As	0.74 ± 0.1	0.4	0.2

The mean co-ordinates of Table 3, but referred to the $P2_12_12_1$ origin (halfway between the three pairs of non-intersecting screw axes), are given in Table 6. There were no unusual features in the final difference maps where residual electron densities varied between about ± 1.5 $e.\text{Å}^{-2}$ and ± 3 $e.\text{Å}^{-2}$. Projections of the structure of conichalcite along [010] and [100] are presented in Fig. 4, where only the oxygen atoms with the specific co-ordinates shown in Table 6 are labelled.

TABLE 6. FRACTIONAL ATOMIC CO-ORDINATES: $P2_12_12_1$ ORIGIN

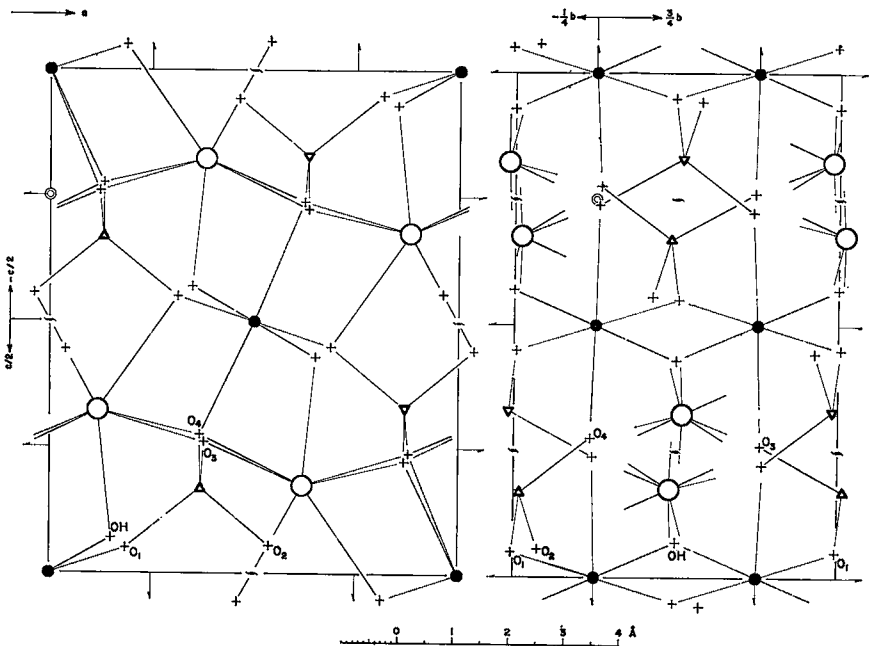| Atom	x	y	z
Ca	0.116_8	0.269_6	0.425_8
Cu	0	0	$\frac{3}{4}$
As	0.368_5	-0.233_2	0.580_6
O$_1$	0.187	-0.256	0.700
O$_2$	0.538	-0.176	0.694
O$_3$	0.378	0.509	0.489
O$_4$	0.368	-0.016	0.474
O$_5$ (OH)	0.151	0.250	0.680

FIG. 4. Projections of conichalcite along [010] and [100]; *Pnma* origin. The $P2_12_12_1$ origin is indicated in each projection by a double circle. Large open circles, Ca; small solid circles, Cu; triangles, As; crosses, O. To avoid confusion, two Cu—O bonds (of an overlapping bipyramid) have been omitted from the centre of the [010] projection, and only the directions of the Ca—O bonds have been indicated (by short lines) in the [100] projection.

DISCUSSION

All As—O, Cu—O, and Ca—O interatomic distances <3 Å are given in Table 7, together with the O—O distances which constitute edges of the co-ordination polyhedra around As, Cu, and Ca. The oxygen co-ordination around As is distorted tetrahedral with the edges given in Table 7, and O—As—O angles of 102°, 103°, 106°, 113°, 116°, and 117° (mean, 109.5°). The oxygen atoms around Cu and Ca are at the corners of a distorted tetragonal bypyramid, and a very distorted "square" antiprism, respectively; the equatorial plane of the former is defined by O_1, O_5(OH), O'_1, O'_5 (OH'), with apices at O_3 and O_4, while the square faces of the latter are represented by O_1, O'_2, O_3, O'_4 and O_2, O_4, O_5 (OH), O_3.

TABLE 7. INTERATOMIC DISTANCES (Å) IN THE THREE TYPES OF
CO-ORDINATION POLYHEDRA

(For each polyhedron, a prime indicates a crystallographically equivalent oxygen atom of the same subscript: ( ), edges shared between As and Ca; [ ], edges shared between Cu and Ca; { }, edges shared between Cu and Cu; ⟨ ⟩, edges shared between Ca and Ca.

	O_1	O_2	O_3	O_4			O_1	O'_1	O_3	O_4	O_5 (OH)	O'_5 (OH')
As	1.74	1.67	1.73	1.60		Cu	2.09	2.04	2.38	2.28	1.95	1.95
O_1		(2.64)	2.77	2.84		O_1			3.22	[3.01]	{2.74}	2.97
O_2			2.89	(2.56)		O'_1			[3.08]	3.15	2.90	{2.74}
O_3				2.78		O_3					3.18	[2.96]
						O_4					[2.97]	3.04

	O_1	O_2	O'_2	O_3	O'_3	O_4	O'_4	O_5 (OH)
Ca	2.54	2.68	2.48	2.53	2.46	2.51	2.54	2.36
O_1		3.33	(2.64)		[3.08]		[3.01]	
O_2			3.15		3.18	(2.56)		
O'_2				3.18		3.71		
O_3						⟨3.07⟩	3.64	[2.96]
O'_3							⟨3.07⟩	2.86
O_4								[2.97]
O'_4								2.93

The atom O_5 can be identified as the OH group with reasonable certainty because it is co-ordinated only with the Ca and (two) Cu cations, and it is the only O not associated with As in the compound anion, AsO_4. It may also be noted that Ca—O_5 and Cu—O_5 are the shortest metal-oxygen distances in the calcium and copper co-ordination polyhedra (see Table 7). Any answer to the question of possible H-bonding between OH and some other O could only be speculative, but it may be mentioned that the only two oxygen atoms not co-ordinated with the same cation are O_5 and O_2, while the separation (2.61 Å) between them (for example,

OH at 0.151, 0.250, 0.680 and the unlabelled O_2 at 0.462, 0.324, 0.806 referred to the $P2_12_12_1$ origin in Fig. 4) is the shortest distance between O_5 and any other oxygen atom, and is suggestive of a H-bond of medium length, and the pertinent angles are Ca (at 0.1168, 0.2696, 0.4258)—OH —O_2 = 122°, Cu (at 0, 0, $\frac{3}{4}$)—OH—O_2 = 104°, and Cu (at 0, $\frac{1}{2}$, $\frac{3}{4}$)— OH—O_2 = 119° (mean, 115°).

The sum of the ionic radii of As^{+5} (0.47 Å) and O^{-2} (1.40 Å) is 1.87 Å but recorded interatomic distances (Wyckoff, 1960) generally are much shorter. For example, regular AsO_4 tetrahedra with As—O distances of 1.62 Å, 1.63 Å,[2] 1.66 Å, 1.73 Å,[3] and 1.75 Å have been reported in $AlAsO_4$, $BiAsO_4$, $BAsO_4$, $YAsO_4$, and KH_2AsO_4, respectively. The tetrahedra in durangite ($NaAlFAsO_4$) are almost regular with As—O = 1.68 Å, while they appear to be very irregular, with As—O = 1.49 Å to 1.81 Å, and 1.59 Å to 1.81 Å, respectively, in the basic arsenates, olivenite ($Cu_2(OH)$ AsO_4) and adamite ($Zn_2(OH)AsO_4$).[4] The As—O bonds in brandtite ($MnCa_2(AsO_4)_2$) have lengths of 1.61 Å, 1.65 Å (two), and 1.76 Å (Dahlman, 1952). Thus, in tetrahedrally co-ordinated arsenic, the As—O bonds appear to fall into two groups, short (approximately 1.59 Å to 1.68 Å) and long (approximately 1.73 Å to 1.76 Å), which are represented in the structure of conichalcite by As—O_4 = 1.61 Å, As—O_2 = 1.67 Å (mean, 1.64 ± 0.03 Å) and by As—O_1 = 1.74 Å, As—O_3 = 1.75 Å (mean, 1.74 ± 0.01 Å), respectively. These distances indicate that the As—O bonds are covalent and hence that they may be compared with the bond lengths to be expected on the basis of the Schomaker-Stevenson equation (Pauling, 1960),

$$D(\text{A-B}) = r_A + r_B - c|x_A - x_B|,$$

where $D(\text{A-B})$ is the length of the bond A-B, r_A and r_B are the covalent radii of atoms A and B, respectively, c is the Schomaker-Stevenson coefficient, and x_A and x_B are the electronegativities of A and B, respectively. Taking r_{As} = 1.21 Å, r_O = 0.74 Å, c = 0.08, x_{As} = 2.0, and x_O = 3.5 (Pauling, 1960), $D(\text{As—O})$ = 1.83 Å for the covalent single bond. This is virtually the same as that (1.84 Å) obtained directly as the sum of the *tetrahedral* covalent radii (r_{As} = 1.18 Å, r_O = 0.62 Å; Pauling,

[2]Assumed on the basis of P—O = 1.56 Å in PO_4, increased by about 3.5% for AsO_4 as deduced from cell volumes of isomorphous arsenates and phosphates of the same cation (Mooney, 1948).

[3]Calculated from the published structural data.

[4]Wyckoff (1960, vol. II, chap. VIII, text pp. 40–41) notes that the very high apparent distortions in olivenite and adamite might perhaps be reduced considerably by further refinement.

1960, p. 246). For the covalent double bond, $r_{As} = 1.11$ Å, $r_O = 0.62$ Å, the other factors remain unchanged, and $D(\text{As—O}) = 1.61$ Å. It is suggested, therefore, that, in the AsO_4 distorted tetrahedra of arsenates, bond lengths of about 1.64 ± 0.04 Å represent essentially covalent double bonds, while those of about 1.74 ± 0.03 Å represent covalent single bonds with some double-bond character.

The AsO_4 tetrahedra, the $CuO_4(OH)_2$ tetragonal bipyramids, and the $CaO_7(OH)$ square antiprisms share edges and corners to form a very tightly-knit three-dimensional network. Each AsO_4 tetrahedron shares two edges (O_1–O_2, O_2–O_4) with separate $CaO_7(OH)$ antiprisms, the corner O_1 also is shared with two $CuO_4(OH)_2$ bipyramids, O_3 is shared with two $CaO_7(OH)$ antiprisms and a $CuO_4(OH)_2$ bipyramid, and O_4 is shared with a second antiprism and a bipyramid. Each $CuO_4(OH)_2$ tetragonal bipyramid shares two O—OH edges with adjacent bipyramids and two others with $CaO_7(OH)$ antiprisms; two O—O edges also are shared with other Ca-antiprisms and all four O corners with AsO_4 tetrahedra. Each $CaO_7(OH)$ square antiprism shares two O—OH and two O—O edges with $CuO_4(OH)_2$ bipyramids, two O—O edges with adjacent antiprisms, and two O—O edges and three additional O corners with AsO_4 tetrahedra. As might be expected, therefore, crystals of conichalcite are relatively dense (specific gravity, 4.33), moderately hard ($\sim$5), and exhibit no cleavage (Strunz, 1939).

As usual with a system of linked polyhedra such as occurs in conichalcite, the shared edges generally are the shortest in a given polyhedron. This is particularly noticeable in the case of the AsO_4 tetrahedron (see Table 7) and here the effect is characteristic of edges which are shared between co-ordination polyhedra involving at least one cation with a relatively high valence number. The decrease in the lengths of the shared edges is less between two Cu-bipyramids, and it is least between two Ca-antiprisms, or between a Ca-antiprism and a Cu-bipyramid. It may also be noted that the O—OH shared edges of the Cu and Ca polyhedra represent the shortest edges of these polyhedra, with the exception of the two O—O edges shared between Ca-bipyramids and the As-tetrahedron. The interatomic distances across the shared edges are As—Ca, 3.19 Å and 3.28 Å; Ca—Ca, 3.95 Å (two); Ca—Cu, 3.39 Å and 3.48 Å (across O—OH), and 3.53 Å and 3.62 Å (across O—O); Cu—Cu, 2.92 Å (two, across O—OH). For comparison, the Ca—Ca distances across shared edges of similar antiprisms in metarossite (Kelsey & Barnes, 1960) are 3.88 Å and 3.91 Å, while the Cu—Cu distances in lindgrenite (Calvert & Barnes, 1957) are 3.15 Å and 3.22 Å across O—OH edges, and 3.01 Å across a shared OH—OH edge, of similar tetragonal bipyramids.

The distorted tetragonal bipyramidal, or octahedral, co-ordination around Cu in conichalcite is similar to that reported in malachite (a basic copper carbonate) by Wells (1951), in lindgrenite (a basic copper molybdate) by Calvert & Barnes (1957), and in linarite (a basic lead-copper sulphate) by Bachmann & Zemann (1961). The equatorial plane consists of alternating O and OH (O—OH—O—OH) in conichalcite, in both non-equivalent bipyramids in malachite, and in one of the two non-equivalent bipyramids in lindgrenite; it consists of adjacent O's and OH's (O—OH—OH—O) in the second bipyramid in lindgrenite, and of four OH (OH—OH—OH—OH) in linarite. The mean Cu—O (or OH) distance in the equatorial plane is 2.01 Å in conichalcite, 1.98 Å and 2.01 Å in malachite, 1.95 Å and 1.97 Å in lindgrenite, and 1.96 Å in linarite. The mean distances from Cu to the apices (O or OH) of the bipyramids is 2.33 Å in conichalcite, 2.41 Å and 2.71 Å (exceptionally long) in malachite, 2.42 Å and 2.46 Å in lindgrenite, and 2.53 Å in linarite.

The eight-fold co-ordination of O in the form of a distorted square antiprism around Ca also occurs in the hydrated calcium vanadate, metarossite (Kelsey & Barnes, 1960), although the degree of distortion is much less than in conichalcite. The corners of the polyhedron are occupied by seven O's and one OH in conichalcite and by five O's and three H_2O's in metarossite. The Ca—O distances vary from 2.36 Å to 2.68 Å (mean, 2.51 Å) in conichalcite and from 2.40 Å to 2.59 Å (mean, 2.46 Å) in metarossite. The shift of Ca and O_2 away from their *Pnma* positions ($y = \pm\frac{1}{4}$) in conichalcite has reduced the Ca—O_2 distances by about 0.5 Å to a value of 2.68 Å, which, although the longest in the co-ordination polyhedron, results in the standard but distorted eight-fold (square antiprismatic) co-ordination of O around Ca. The displacement of As may then be considered as the result of a tendency to reduce distortion, and relieve strain, in the AsO_4 tetrahedron.

The structures of descloizite and pyrobelonite may be expected to be basically the same as that of conichalcite. A very few non-*Pnma* reflections have been observed from descloizite (Qurashi & Barnes, 1954, p. 420), but none were recorded from pyrobelonite at the time of the investigation of its structure (Donaldson & Barnes, 1955). Refinement of the descloizite structure in $P2_12_12_1$ will be described in a separate paper, where the results will be discussed in relation to those for pyrobelonite and conichalcite.

REFERENCES

BACHMANN, H. G. & ZEMANN, J. (1961): Die Kristallstruktur von Linarit, $PbCuSO_4(OH)_2$, *Acta Cryst.*, **14**, 747–753.

BARNES, W. H. & QURASHI, M. M. (1952): Unit cell and space group data for certain vanadium minerals, *Am. Mineral.*, **37**, 407–422.

BERRY, L. G. (1951): Observations on conichalcite, cornwallite, euchroite, liroconite and olivenite, *Am. Mineral.*, **36**, 484–503.

CALVERT, L. D. & BARNES, W. H. (1957): The structure of lindgrenite, *Can. Mineral.*, **6**, 31–51.

CRUIKSHANK, D. W. J. (1949): The accuracy of electron-density maps in x-ray analysis with special reference to dibenzyl, *Acta Cryst.*, **2**, 65–82.

DAHLMAN, B. (1952): The crystal structures of kröhnkite, $CuNa_2(SO_4)_2.2H_2O$ and brandtite, $MnCa_2(AsO_4)_2.2H_2O$, *Ark. Min. Geol.*, **1**, 339; see *Structure Reports for 1952*, Oosthoek, Utrecht, **16**, 289–292 (1959).

DONALDSON, D. M. & BARNES, W. H. (1955): The structures of the minerals of the descloizite and adelite groups: II—pyrobelonite, *Am. Mineral.*, **40**, 580–596.

FREEMAN, A. J. (1959): Atomic scattering factors for spherical and aspherical charge distributions, *Acta Cryst.*, **12**, 261–271.

KELSEY, C. H. & BARNES, W. H. (1960): The crystal structure of metarossite, *Can. Mineral.*, **6**, 448–466; (1961): *loc. cit.*, **6**, 697.

MOONEY, R. C. L. (1948): Crystal structure of tetragonal bismuth arsenate, $BiAsO_4$, *Acta Cryst.*, **1**, 163–165.

PAULING, L. (1960): *The nature of the chemical bond*, Cornell, Ithaca.

QURASHI, M. M. (1963): Use of the anti-symmetric component of the Patterson and Fourier functions for the solution of problems involving small atomic shifts from positions of super-symmetry, *Acta Cryst.*, **16**, 307–310.

QURASHI, M. M. & BARNES, W. H. (1954): The structures of the minerals of the descloizite and adelite groups: I—descloizite and conichalcite (part 1), *Am. Mineral.*, **39**, 416–435.

QURASHI, M. M., BARNES, W. H., & BERRY, L. G. (1953): The space group of conichalcite, *Am. Mineral.*, **38**, 557–559.

STRUNZ, H. (1939): Mineralien der Descloizitgruppe. Konichalcit, Staszizit, Austinit, Duftit, Aräoxen, Volborthit, Pyrobelonit, *Zeit. Krist.*, (A) **101**, 496–506.

WATSON, R. E. & FREEMAN, A. J. (1961): Hartree-Fock atomic scattering factors for the iron transition series, *Acta Cryst.*, **14**, 27–37.

WELLS, A. F. (1951): Malachite, re-examination of crystal structure, *Acta Cryst.*, **4**, 200–204.

WYCKOFF, R. W. G. (1960): *Crystal structures*, Interscience, New York.